

Article

# Nano Porous Zinc Synthesis on Soft Polyurethane Foam Using Conductive Ink and Electroplating Method

Mehdi Salimi <sup>1</sup>, Seyed Mohammad Mousavi Khoiee <sup>1</sup>, Eskandar Keshavarz Alamdari <sup>1,\*</sup>, Milad Rezaei <sup>1</sup> and Maryam Karbasi <sup>2</sup>

<sup>1</sup> Department of Materials and Metallurgical Engineering, Amirkabir University of Technology (Tehran Polytechnique), Tehran 15875-4413, Iran

<sup>2</sup> Department of Materials Engineering, Isfahan University of Technology, Isfahan 83111-84156, Iran

\* Correspondence: alamdari@aut.ac.ir; Tel.: +98-2164542971

**Abstract:** High specific surface is a significant characteristic in zinc coatings that can be highly applicable in batteries and catalysts. Conventional methods to create foams are not cost-efficient, nor could they make a high specific surface. Electroplating has been developed that can produce a very high specific surface foam. On the other hand, conductive ink can create an affordable conductive surface with a high specific surface, so the study on using conductive ink, which has a cost-efficient nature, was necessary to create a conductive surface. This work has investigated the effect of crucial parameters, such as graphite size, coating time and bath composition, on the current efficiency and SEM microstructure. As a result, a 3  $\mu\text{m}$  graphite size was found to be appropriate. Coated zinc escalates linearly with current efficiency for up to 5 h, and then it decreases. Although the zinc concentration increases up to 0.12 mol/L in the electrolyte, making a slight increase in loading, the current efficiency was almost unchanged. However, if it increases more, the loading and current efficiency significantly rise so that the loading grows up to 16 times and the current density increases up to 86%. Additionally, the morphology changes from dendritic to compact plates, sphere and semi-sphere, subsequently.

**Keywords:** zinc nanoparticle; nano pores; conductive ink; zinc foam; specific surface area



**Citation:** Salimi, M.; Mousavi Khoiee, S.M.; Keshavarz Alamdari, E.; Rezaei, M.; Karbasi, M. Nano Porous Zinc Synthesis on Soft Polyurethane Foam Using Conductive Ink and Electroplating Method. *Metals* **2022**, *12*, 1945. <https://doi.org/10.3390/met12111945>

Academic Editors: Chih-Ming Chen, Norman Toro, Edelmira Gálvez and Ricardo Jeldres

Received: 15 August 2022

Accepted: 5 November 2022

Published: 13 November 2022

**Publisher's Note:** MDPI stays neutral with regard to jurisdictional claims in published maps and institutional affiliations.



**Copyright:** © 2022 by the authors. Licensee MDPI, Basel, Switzerland. This article is an open access article distributed under the terms and conditions of the Creative Commons Attribution (CC BY) license (<https://creativecommons.org/licenses/by/4.0/>).

## 1. Introduction

The production of light materials with high efficiency in the battery and catalyst production industry has been the focus of various materials engineering research topics. One of these cases is the synthesis of catalysts, cathodes and anodes of batteries. As is known, the reaction surface plays a key role in heterogeneous reaction kinetics, so it can be achieved by using processes that create a high specific surface area. At the same time, production costs have been diminished due to the reduction of consumables [1–3]. The development of nanotechnology and nanomaterials leads to create a vast surface of reaction that have been used in various industries [4].

Various methods, including methods of synthesis from melt [5], the use of metal vapor with vapor deposition [2,6,7], powder metallurgy [8–10], and electrochemical methods [11], have been proposed for making cellular solid [12] and metal foams [13,14]. Among these methods, some are able to produce open-cell foams, and some are suitable for closed-cell foams. The method of using a metal melt to create zinc foam, synthesized by adding  $\text{ZrH}_2$  to the zinc melt, creates closed porosity foams that do not have a very high specific surface area [5]. Using  $\text{TiH}_2$  and  $\text{ZrH}_2$  melt method, zinc foams with porosity of 81 to 92% with closed porosity were obtained [15]. One of the methods used to create high porosity metal foams is to apply a coating on polyurethane foams. This coating can be generated by various methods, such as conductive ink containing graphite. After conducting the foam surface by conductive ink, a nickel coating was applied by electroplating method resulting

foams with 98% porosity [16–19]. In addition, zinc foams or fibers, which are attained from electroplating process, are used as anodes for batteries that can expand battery lifespan [20]. Therefore, the zinc fibers achieved by pouring molten zinc onto the turntable generally were exploited in the battery anodes, in which the special surface of the anode plays a crucial role in the anode's efficiency [17]. In another study, zinc coating on the surface of polyurethane foam was created after degreasing, acid washing, and activating the foam surface. In this way, first, the electroless copper coating was applied, and then the surface of the foam was coated by electroplating in zinc sulfate solution, which creates a porosity of more than 90% [21].

Battery life extension by increasing the specific surface area of the battery's anode encouraged the application of dendritic zinc anodes with a higher specific surface area. These anodes are obtained by electroplating zinc with a specific surface area of about 12 square meters per gram. Moreover, the size of nanoparticles synthesized in this method is reported to be 54 to 96 nm, which has accelerated the reaction rate by increasing the effective surface area by 10 to 25 times compared to normal anodes [1]. The use of zinc foams created by the method of stabilizing suspended zinc powder particles, which have become solid foam, is also one of the proposed methods for creating this type of anode, which is used to create porosity. The volume of pores is about 220 mm<sup>3</sup> per gram, with pores diameter ranging from 8 nm to 20 μm [3].

Hyper dendritic zinc coating, which is achieved by electroplating zinc sheets using a bath containing KOH, ZnO, and H<sub>2</sub>SO<sub>4</sub> electrolyte, positively affects battery lifespan [22]. Conductive graphite is used as a zinc metal host by electrolytic zinc plating to achieve a suitable active surface for battery anodes. This coating is applied to graphite fiber in a bath containing sodium sulfate and zinc sulfate. In this process, the annealing of graphite fibers is done to create hydrophobicity. Unfortunately, the surface properties such as specific surface area, coating morphology, or particle size has not been reported, and only the attributes of the generated battery were measured [23]. A type of copper alloy foam has been used as the electrode, which has been obtained by electroplating, to create a catalyst for electrochemical reduction of carbon dioxide [24]. A bath containing zinc sulfate, sulfuric acid and copper sulfate was used to create this alloy foam [24]. The depth of pores created by this method, is six to 16 μm [24], and the size of zinc particles is 30 to 50 nm [25], respectively. Additionally, dendritic zinc electroplated on silver has been used as a catalyst for the conversion of carbon dioxide to methanol, the achieved foam has micron-sized pores [26]. Zinc foam is also created by the suspension of zinc powder particles in emulsions containing carboxymethylcellulose, sodium dodecyl sulfate, decane and water to create zinc-air batteries anode. The resulting zinc particles, which lacked zinc oxide, were first dried at 120 °C and then sintered at 409 °C in an argon gas stream. The sponge is raised, but no research has been conducted on the shape, size, and active surface area [27].

The electroplating of zinc on copper and nickel foams has been studied at a constant current density. Electron microscopy images showed zinc-like coatings formed on the surface of the foams, which can have an immense specific surface area [28]. The specific surface area obtained from the electrolytic plating process is significant, but first, an appropriate conductive surface must be provided to create multiple layers. The use of costly processes such as conducting a conductive surface by plastic plating methods will make the coating more expensive, so affordable processes should be considered to create a conductive base coating. One of these methods is the utilization of graphite and graphite inks as conductors [28]. The conductive ink was investigated to create a conductive coating on paper for RC circuits, in which the steps of preparing the graphite-based conductive ink were investigated for a fully conductive layer with low electrical resistance [28]. Very cheap commercial graphite powder is used to reduce the cost of the conductive layers. However, the size of graphite particles, which greatly affects conductivity, has not been reported [29]. On the other hand, the idea of using graphite-based conductive ink was developed by using a mixture of carbon black and graphite with a size of 17 μm. The lowest electrical resistance was achieved when the weight ratio of graphite to carbon black was 1.8 [30].

In this research, an attempt has been made to develop a method of using conductive ink to create inexpensive foams and to achieve surfaces with a very high specific area using conductive ink and electrolytic coatings on the conductive surface. Unlike previous studies, the effect of graphite particle size on the foam's properties has been investigated. Moreover, crucial parameters of the plating bath such as time, zinc concentration, zinc acetate, and acetic acid concentration are investigated. On the other hand, attempts will be made to obtain structures with high specific surface area and nanometer cavities to create more reaction sites.

## 2. Materials and Methods

### 2.1. Materials

Two types of polyurethane foam were used in this research, one with high density with  $0.05 \text{ g/m}^3$  and another with lower density with  $0.035 \text{ g/cm}^3$ . Foams were washed and degreased by 96% ethanol (Merck product) and 5% caustic soda (Merck product) solution, respectively. In addition, the foams were subsequently washed by 1% sulfuric acid (Dr. Mojallali Industrial Chemical Complex Co., Kaveh Industrial City, Saveh, Iran) solution and then etched with potassium permanganate (Merck KGaA, Darmstadt, Germany). Commercial conductor graphite powder (made by Nirou Seraj Industrial Carbon Brushes Co., Tehran, Iran) and commercial liquid sodium silicate (glass water made by Zarin water glass Co., Qazvin, Iran) were used to make conductive ink. Graphite particles were crushed by a mixer mill, and subsequently, the size of graphite particles was measured by a laser particle size analyzer as far as the suitable size of graphite was achieved for optimum conduction of the ink. Thus, the optimum size of graphite powder was considered to be  $3 \mu\text{m}$  which then was used for the main tests. In addition, the conductor ink was made by adding 50 g of graphite powder to 250 mL of water and adding 5 g of liquid sodium silicate adhesive, which was stirred on a magnetic stirrer for 24 h before homogenizing the ink at ambient temperature.

### 2.2. Methods

Since the formation of porous metal requires the main substrate to be light and of high porosity, the electrolyte can easily pass through it and settle on the foam surface. Various types of foams, including polyethylene foams, poly sponges high-density urethane and low-density foams were tested for coating, but the surface of high-density foams was closed quickly during coating, and surface closure prevented electrolyte penetration, so the plating process was interrupted. Thus, low-density foams were better in practice, so two types of polyurethane foam were used, one of which had a density of  $0.05 \text{ g/cm}^3$ , and the other had a density of  $0.035 \text{ g/cm}^3$ . First of all, foams were cut to dimensions of  $10 \times 10 \times 10 \text{ mm}$ , their weight was measured and recorded with a scale weighting  $0.001 \text{ g}$  Kern KB360 and then washed in ethanol for 10 min and dried in ambient atmosphere. The sample was placed in a degreasing solution for 10 min after it was rinsed with distilled water. Next, it was placed in an etching solution for 10 min, washed with distilled water, and dried in the ambient atmosphere. Next, the copper wire was connected to the foam and it was immersed in the conductor ink solution for half an hour. It was then dried in an oven at  $100 \text{ }^\circ\text{C}$  for 3 h, its resistance was measured from the wire head to the end of the foam. If this resistance was less than  $100 \Omega$ , it was useable for sequence tests; otherwise, the immersion operation should have been repeated.

To apply the coating on graphite-coated foams connected to copper wire, they are placed in the bath and connected to the cathode. the commercial pure 99.98% zinc sheet product of Kholes Sazan zinc production Company was used as the anode. A magnetic stirrer gently stirred the bath and its pH was dynamically measured by a pH meter of Metrohm (Model 780) and kept constant with a solution of caustic soda and sulfuric acid solution.

The foams in the same conditions were coated in a bath containing 10% acetic acid solution and 25 g/L of sodium sulfate for one hour and then analyzed for uniformity,

adhesion, and coating quality. After the electrodeposition process, the sample was washed in distilled water, dried in an oven, and then weighed. The composition of the bath and the conditions of electroplating are listed in Table 1.

**Table 1.** The composition of the bath and the conditions of electroplating are listed.

Test No.	Current Density A/cm <sup>2</sup>	Na <sub>2</sub> SO <sub>4</sub> gr/L	Acetic Acid Vol. Percent	Coating Time H	Zinc Acetate Mol	Bath Vol. L	Description
1	0.2	25	10%	1	0	0.4	Coating time
2	0.2	25	10%	2	0	0.4	Coating time
3	0.2	25	10%	3	0	0.4	Coating time
4	0.2	25	10%	4	0	0.4	Coating time
5	0.2	25	10%	5	0	0.4	Coating time
6	0.2	25	10%	6	0	0.4	Coating time
7	0.2	25	10%	10	0	0.4	Coating time
8	0.2	25	10%	3	0.076	0.4	Zinc effect
9	0.2	25	10%	3	0.115	0.4	Zinc effect
10	0.2	25	10%	3	0.136	0.4	Zinc effect
11	0.2	25	10%	3	0.272	0.4	Zinc effect

A series of tests were carried out to achieve the optimal coating time so that the highest current efficiency with the highest coating porosity is produced. The foam preparation and bath composition used were considered as current density experiments. With the difference that all experiments were performed on the optimized current density in the previous experiment. In this part, the tests were performed from one hour to 10 h from the time of coating and its effect on the current efficiency, weight, and quality of the coating (no shedding, adhesion, and non-etching of the foam coating) was investigated.

The composition of the bath and its effect on the coating applied on the foam should be investigated. The parameters under study include the effect of zinc concentration, acetic acid concentration and zinc acetate concentration. Each of these parameters were investigated at three different levels and their effect on current efficiency and coating weight was measured.

One of the most important parameters under study is the effect of zinc concentration in the plating bath on the quality of the coating. This effect was studied using adding pure zinc acetate made by Merck company and dissolving in the bath, which was done in zinc concentration 0, 0.076, 0.115, 0.136, and 0.272 mol/L. The atomic absorption method was used for chemical analysis. The complementary method of titration has been used for investigations. The results obtained from these two analyses confirmed each other.

The morphology, structure, and quantitative analysis of the coating are of critical importance and affect the quality of the foam and its specific area. Olympus optical microscope (model BX53) and scanning electron microscope (FEI ESEM QUANTA 200) were used to examine the shape, morphology, and quantitative analysis of the coating.

To eliminate the effect of current density in all tests, the current density was chosen to be a constant parameter. The current density of electrodeposition was set to 0.2 A·cm<sup>2</sup> cross section of the foam, for the surface is etched at higher current densities and also does not have the required specifications, such as adhesion to the foam surface, non-etching, strength, non-powdering, and non-destruction of sediment, etc. At lower current densities, the coating rate was very low. For this reason, in the tests performed, the current density was used, which had the best properties in terms of the mentioned parameters.

### 3. Results

#### 3.1. Graphite Particle Size Effect

After crushing the graphite, the size of the graphite particles was checked by a laser particle size analyzer in order to obtain the appropriate size. Figure 1 represents the effect of crushing time on graphite particle size, as observes, crushing graphite has reduced the

size of graphite. Additionally, Figure 1 illustrates the effect of crushing time on the specific surface of graphite powder. It can be seen that increasing the crushing time leads to a specific surface rise.

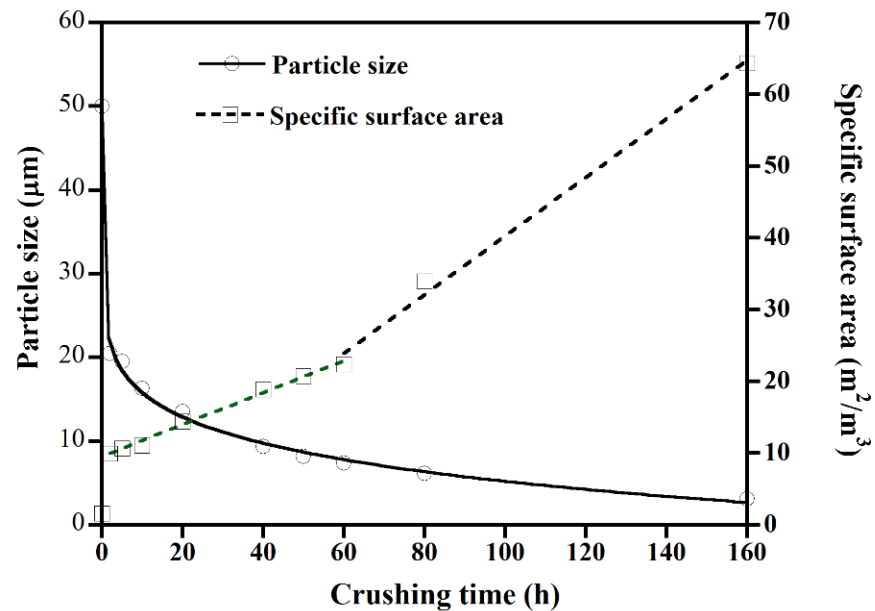


Figure 1. Diagram of the effect of crushing time on graphite particle size and specific surface area.

### 3.2. Effect of Particle Size on Ink Conductivity

The effect of graphite particle size on conductivity is shown in Figure 2. It is observed that the conductivity improved by reducing the graphite particle size. The conductivity increase in the presence of polyurethane is more than in paper and polyethylene.

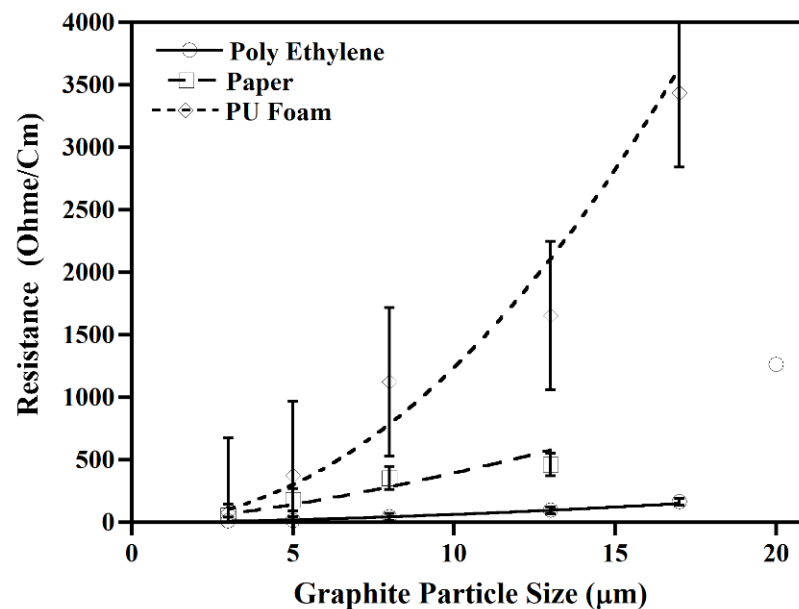


Figure 2. Effect of graphite particle size on the conductivity of ink applied to paper, polyethylene, and polyurethane foam.

### 3.3. Zinc Coating Results

In Figure 3, the coating weight results relative to the foam's initial weight are plotted versus the application time of the coating. This curve is s-shaped and includes the nucle-

ation, growth, and end stages. Additionally, visual observations during the process, shows the accumulation and release of hydrogen ions on the surface. In Figure 4, the current efficiency curve is plotted in terms of coating time. The increase in efficiency up to the first 4 h then a drop-in efficiency rate (curved region) after the linear region can be observed. Figure 5 indicates EDS analysis results with an electron microscope image for a sample electroplated for 10 h, which shows the formed phases, including zinc and zinc oxide. Figure 6 shows electron microscope images of zinc deposits corresponding with samples 3, 4, 5, 6, and 10 h. As can be seen, the coating is created in the form of a sheet with enormous of coating. Additionally, holes with a size of nanometers are observed.

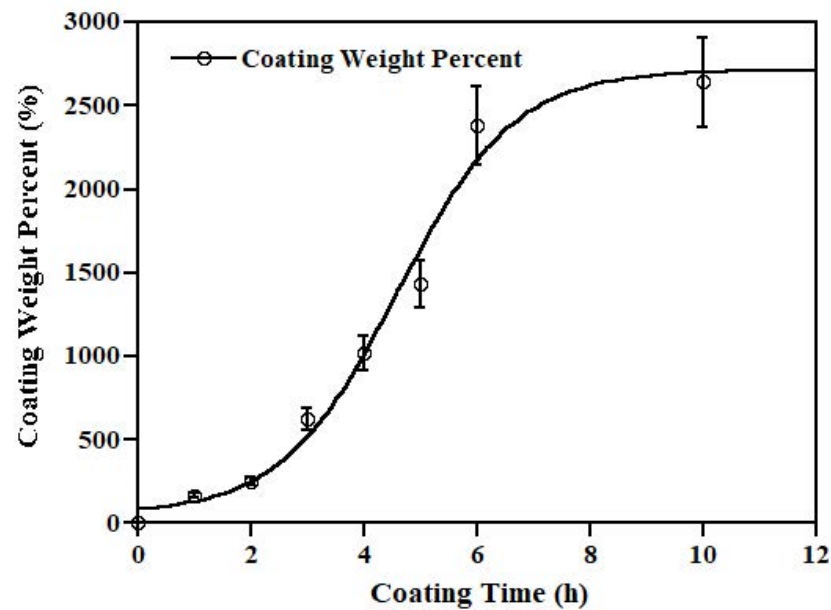


Figure 3. The results of the applied coating weight relative to the initial weight of the foam are plotted as a percentage of the coating application time.

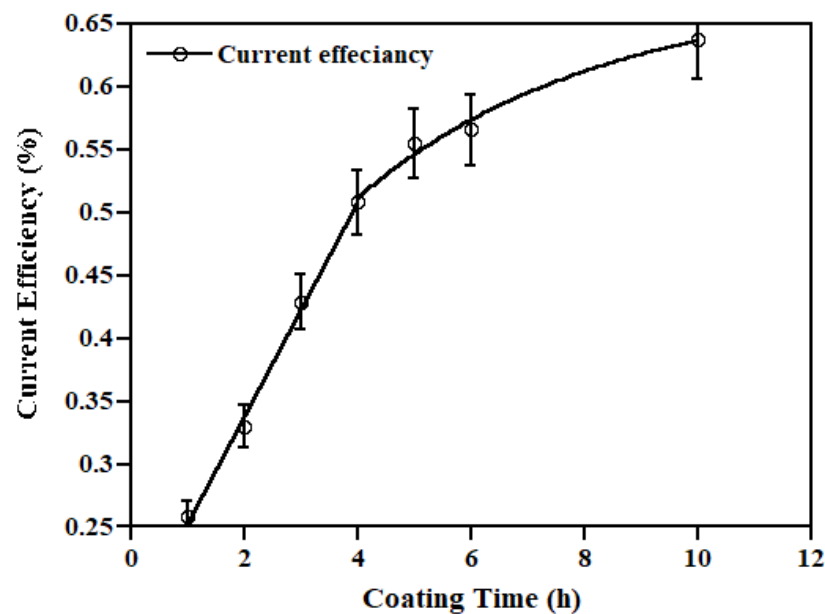
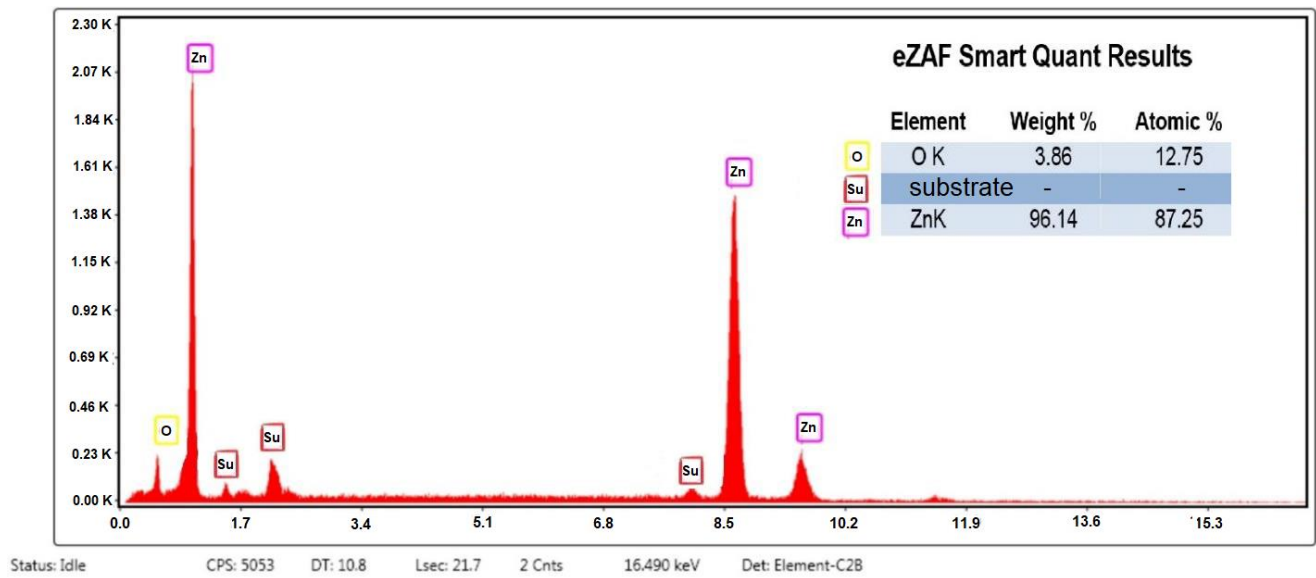
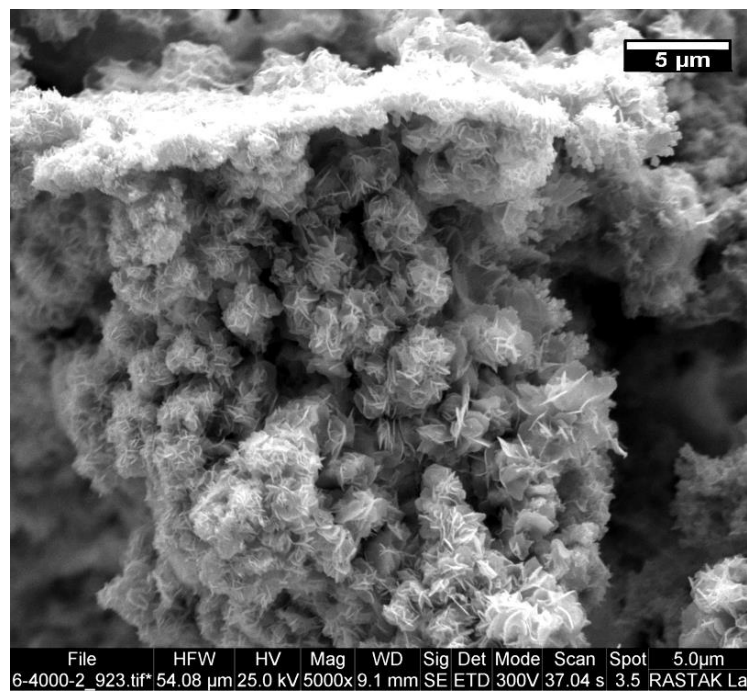


Figure 4. Shows a current efficiency diagram drawn in terms of coating application time.

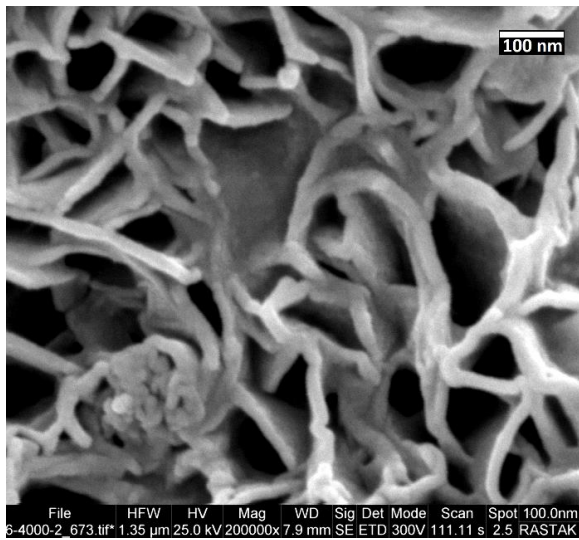


(a)

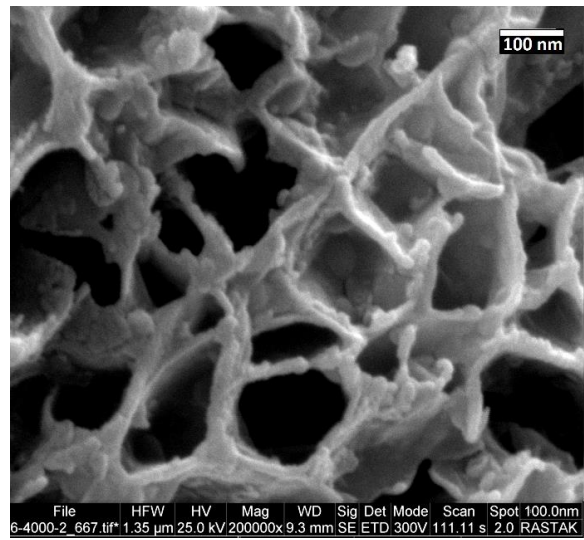


(b)

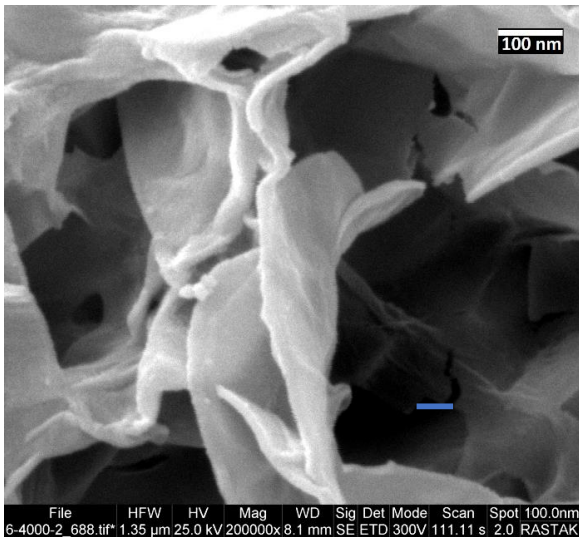
**Figure 5.** (a) EDS test results with an electron microscope for a sample of 10 h electroplated (sample 7), which shows the formed zinc and oxygen. (b) SEM photo from area which EDS was taken.



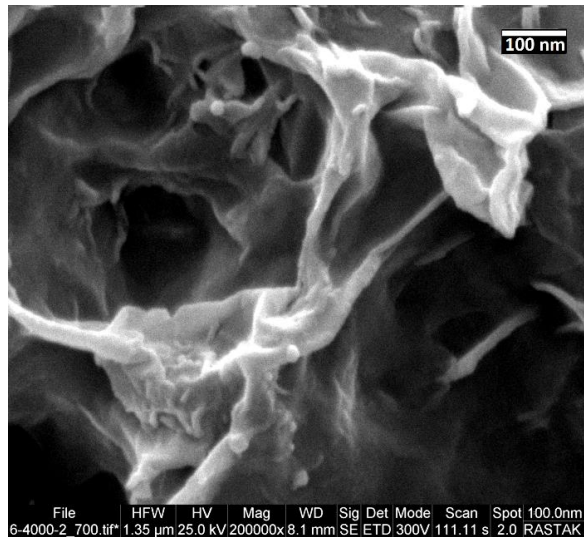
(a)



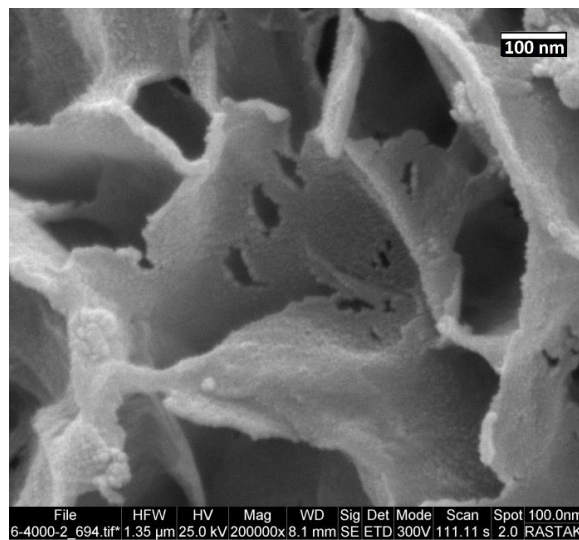
(b)



(c)



(d)



(e)

Figure 6. SEM photos related to electroplated for: (a) 3 h, (b) 4 h, (c) 5 h, (d) 6 h, (e) 10 h.

### 3.4. The Effect of Zinc in the Bath

Various types of zinc compounds are added to the plating bath to investigate the effect of zinc species on coating quality. First, zinc acetate was added to the bath, which had an intensely positive effect on the weight of the coating. The diagram of the impact of increasing zinc is shown in Figure 7. It was observed that in the bath, there is no dendritic zinc sediment, nor the obvious effect of adding zinc is recognized on the loading and current efficiency. Moreover, the coating structure becomes more compact with a gradual increase in zinc deposition, and the plates stick together. With the additional increase of zinc concentration, both the current efficiency and loading rate increase, and the structure becomes spherical. The further growth of zinc coating makes a semi-spherical structure. Since this study aimed to obtain a higher specific surface area, but the addition of zinc compounds reduces the specific surface area, its addition was not considered appropriate. However, the effect of zinc species concentration on the microstructure seems very interesting to be evaluated in later studies.

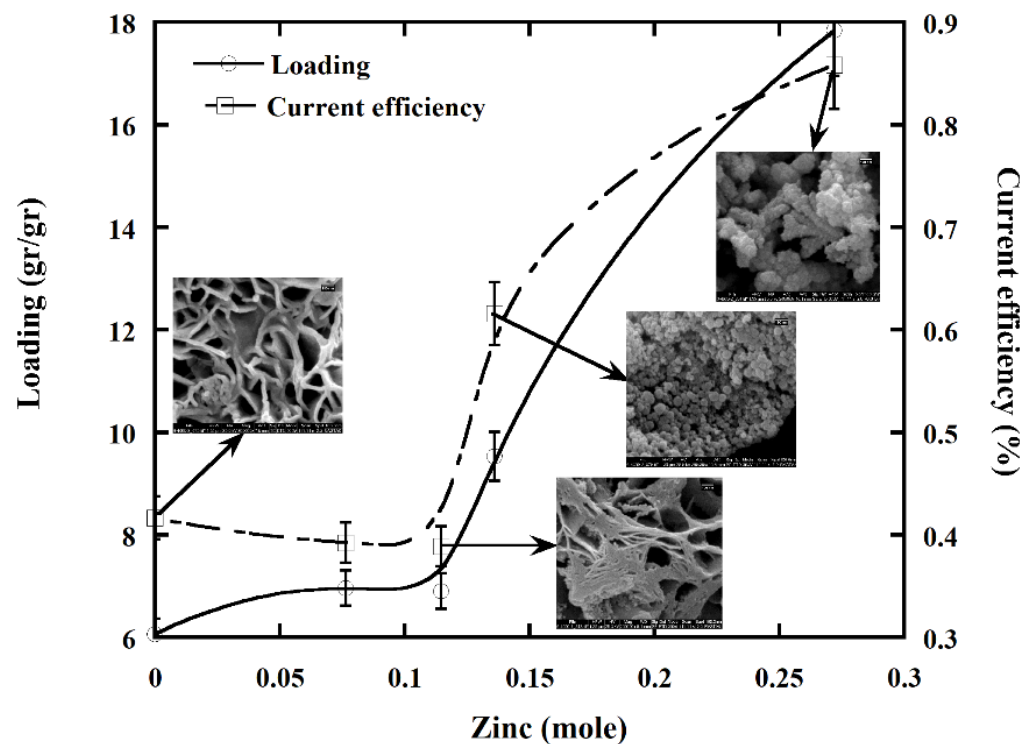


**Figure 7.** Shows the loading and current efficiency versus the amount of zinc mole on the bath for 3 h coating time. In each section, the structure of the electron microscope Image corresponding to that section is given at the top.

## 4. Discussion

### 4.1. Graphite Particle Size Effect

Figure 1 represents the effect of crushing time on graphite particle size. As reported in other works [31,32] grinding graphite has reduced the size of graphite; on the contrary, in some studies, the particles have agglomerated, and the size has increased during the milling process [33]. This difference is due to the fact that ball mills make an agglomeration of graphite particles [34] that can be reduced by using the shear mills [35]. Hence, the ice-breaker program is used at the mixer mill apparatus, which crushes the graphite particles with high power and a sharp stainless-steel blade, so that aggregation does not happen. With regards to the effect of crushing time on the specific surface of graphite powder (Figure 1), increasing the specific surface area confirms previous reports [30–34].

#### 4.2. Effect of Particle Size on Ink Conductivity

The effect of graphite particle size on conductivity is shown in Figure 2. Although no record has been found to survey the effect of particle size on the conductivity, it is observed that the conductivity can be improved by reducing the graphite particle size. However, since the creation of a single layer of graphite in a structure similar to graphene creates a much higher conductivity, it can be said that a similar effect may also be created here, although the size and shape of the particles are far from reaching the size and shape of graphene [36,37]. It is suggested that in future research, the effect of graphene formation on electrical conductivity should be investigated more carefully. Here, no claims are made about the obtained evidence and only the results of other researchers are mentioned.

#### 4.3. Zinc Coating Results

This curve (Figure 3) is s-shaped and includes the nucleation, growth, and end stages. In the nucleation stage, the formation of zinc coating on the foam surface is happening at a low speed because of the low conductivity of the conductive ink, which has caused a low coating rate. On the other hand, most of the applied energy is spent on hydrogen reduction, and the current is wasted in the initial stage. In the competition for electron adsorption,  $H^+$  has a better chance than  $Zn^{2+}$  to reduce more on the surface graphite. Additionally, visual observations during the process confirm the accumulation and release of hydrogen ions on the surface. Because graphite is an excellent catalyst for hydrogen reduction and release, most of the applied current is spent on hydrogen reduction and less on zinc. [38,39] Thus, in the initial steps of the electrodeposition process, hydrogen release diminishes current efficiency in Figure 4. After the coating is formed on the entire surface of the foam, the conductivity is greatly increased, so the coating rate increases, which makes the growth step. Due to the formation of the zinc layer on the graphite surface, the nucleation of hydrogen bubbles on the zinc surface is difficult. As a result, the current efficiency increases, so more current employs for zinc reduction instead of hydrogen reduction, and zinc coating grows faster.

The exchange current density on the zinc surface for the hydrogen release reaction is about  $10^{-10}$  A/m<sup>2</sup>. The degree of polarization, due to the hydrogen gas release, is low, and most of the applied current is spent on the deposition of zinc on the foam surface [40,41]. As a result, the loading increases by creating a zinc coating on the foam surface. In the final stage, the deposition rate decreases again, for the sediment porosity is very high, as was observed in electron microscopy results. A concentration gradient is created through the spaces inside the porosity that decline the current efficiency.

On the other hand, the hydrogen emission in solution due to polarization decrease the hydrogen ions concentration. Consequently, while pH rises, the value of sediment zinc at the cathode surface has reduced. Increasing the pH at the front of the coating surface causes the deposition of zinc hydroxide. The formation of zinc hydroxide creates an insulating layer and prevents the continuation of the deposition process. Figure 3 shows the zinc reduced value over time. The decrease in zinc weight percent can be due to the reduction of zinc reduction efficiency. As shown in Figure 4, by increasing the time, the efficiency of the cathodic reduction of zinc decreased significantly. The decrease in zinc reduction can be the release of hydrogen gas evaluation on the surface instead of zinc. Therefore, it is expected that with increasing time, the value of hydrogen ions in front of the surface of the cathode will decrease drastically, and due to the increase in pH value, according to the curve, the possibility of zinc hydroxide sedimentation will increase. In this situation, using a technique that can confirm the presence of oxygen on the surface can be very useful. The X-ray technique is utilized to identify different phases. However, since the amount of oxide or hydroxide formed at the surface in comparison to the deposited metal is much less than 5%, it is practically impossible to detect this phase. Therefore, another method should be used to detect this compound in very small amounts. One of the most efficient techniques that can be used in this field is the EDS or XPS method.

The detection of hydrogen is essentially impossible by a lab-based EDS or XPS. Recruitment of a technique that correctly proved the existence of oxygen may be used for the presence of zinc hydroxide compounds as evidence. By using the EDS method, the presence of oxygen in the surface layer can be detected in a much simpler and more economical way. Figure 5 indicates EDS analysis results with an electron microscope image for a sample electroplated for 10 h, which shows the formed phases, including zinc and oxygen. The formation of the insulating oxide layer causes the possibility of the growth of new sediment to decrease in the places where this layer is formed. As a result, the current efficiency, and the rate of zinc reduction, decrease.

The increase in efficiency up to the first 4 h (Figure 4) can be attributed to a rise in the reaction rate due to the creation of new coatings surfaces that develop the surface's conductivity. A drop-in efficiency rate after the linear region can be attributed to the coating falling after 4 h and the instability of the layer.

Electron microscope images (Figure 6) show that the thickness of the zinc plates decreases. After 4 h, the size of the pores increases, and the thickness of the walls decreases. As can be seen in Figure 6a, there is probably a relatively large surface area available during the formation of initial deposits on the surface of the foam. In these conditions, the concentration of zinc in the solution is relatively high. As a result, the electro-reduced zinc plates are formed close to each other and get a chance to grow very thick. With the progress of the reaction, the polarization causes a decrease in the concentration of zinc inside the cavities, and the late-formed zinc deposits are built on the previous surfaces. Due to the lack of zinc inside the cavities, the created plates grow in the form of dendrites toward the middle of the solution. Fast dendritic growth reduces the thickness of the new deposit wall. In this case, if new nuclei are formed on the previous surfaces, they will have less chance to grow due to the low concentration of zinc. As can be seen in Figure 6b–e, since the place of nucleation of these dendrites is on the outer surface of previous plates, there is little space for this nucleation the walls become thinner. Because zinc penetration to the inner side of pores is slow, surfaces grow in the direction where zinc is more accessible. Therefore, in the progress of the process, the size of the new holes gets bigger. Due to the length of this article, statistical reviews, electron microscopy, and BET results will be presented in another article later.

Based on observations, the increasing time of more than 4 h, the strength of the foam gradually decreases. So, the value of the fallen part of foam during the process increases. Due to the formation of thin deposits on the thin dendrite layer and its rapid growth towards the solution, the regenerated particles do not have the necessary strength and are then easily torn off due to their weak connections.

#### *4.4. The Effect of Zinc in the Bath*

It seems that concentration polarization causes the dendritic structure on the surface. Concentration polarization declines metal concentration around the cathode, so the sediment moves away from the cathode surface and grows into the solution bulk to absorb zinc species. Increasing the polarization effect changes the sediment structure. With a further increase of zinc concentration in the bath, the impact of concentration polarization decreases, and a spherical structure is created. Finally, a hemispherical structure is formed. Current efficiency and deposition rate rises due to zinc concentration increment that reduces the concentration polarization in the solution, and increased efficiency, which is entirely consistent with the results. This has also been seen in the electroplating of various metals. By increasing the metal concentration in the solution, the uniformity of the coating increases, and better surface smoothness obtain. Based on the results obtained as reported, this issue applies here as well.

## **5. Conclusions**

Graphite particle size plays a critical role in conducting conductive ink, increasing with decreasing particle size. Based on the observations, increasing the graphite crushing

time, the particle size is dramatically reduced at first, and after 40 h, the particle size changes are insignificant. This is even though the specific surface area of crushed graphics increases steadily from 18.9 to 64.4 m<sup>2</sup>/m<sup>3</sup> between 40 and 160 h. The suitable particle size of graphite was found equal to 3 microns. Using this size of graphite can increase the electrical resistance to below 100 ohms/cm on the surface of the foam. Polyurethane foam, which surface has been conducted with conductive ink, can provide a porous zinc coating with nanometer-thick sheets by electrodeposition in an acetic acid solution. By coating the surface of this foam for up to 4 h, regular efficiency and acceptable speed for applying the coating are obtained. Increasing the rate of zinc reduction on the surface causes the formation of dendrites that enhance rapidly. The electro-reduction method was used to deposit zinc on the polyurethane surface. The decrease in zinc sedimentation can be due to the depletion in zinc reduction efficiency and the resuscitation of hydrogen. In addition, the formation of the insulating oxide layer causes the possibility of the growth of new sediment to decrease in the places where this layer is formed. Electron microscopy images show that by increasing time, the microscopic structure of deposited zinc changes, and thinner partitions with larger pore sizes are obtained instead of thicker walls. Due to the weak connection of the plates formed in these conditions, the obtained structure will have low strength. Adding zinc acetate to the bath converts the shape of the sediments from sheets to spheres with nanometer size. Adding zinc acetate to the bath, the morphology of the sediment changes from sheet to adhesive sheets, and in some areas, these sheets are thoroughly compressed by adding more zinc, and the morphology of the sediment changes to spherical and hemispherical. To achieve a high specific surface area, according to the morphology, non-compressed sheets are preferred, so using a bath with low zinc acetate can lead to a high specific area. The foam with a proper specific surface, strength and current efficiency is prepared between 4 and 6 h. The results obtained from this research show that the obtained levels can be used as acceptable levels for the process of cementation of impurities such as nickel and cadmium from an aqueous media containing zinc. Our supplementary research regarding the statistical reviews, electron microscopy, and BET results will be presented in another article.

**Author Contributions:** M.S., investigation, methodology, chemical, formal analysis and data curation, funding acquisition, writing the original draft; S.M.M.K., supervision; E.K.A., supervision, conceptualization, methodology, data curation, review and editing; M.R., supervision; and M.K. supervision, formal analysis and data curation, review and editing. All authors have read and agreed to the published version of the manuscript.

**Funding:** This research received no external funding.

**Data Availability Statement:** Restrictions apply to the availability of these data. Data were obtained from Amirkabir University of technology and are available from Eskandar Keshavarz Alamdari with the permission of Amirkabir university of technology.

**Conflicts of Interest:** The authors declare no conflict of interest.

## References

1. Chamoun, M.; Hertzberg, B.J.; Gupta, T.; Davies, D.; Bhadra, S.; Van Tassell, B.; Erdonmez, C.K.; Steingart, A.D. Hyper-dendritic nanoporous zinc foam anodes. *NPG Asia Mater.* **2015**, *7*, e178. [[CrossRef](#)]
2. Drieschner, S.; Weber, M.; Wohlketter, J.; Vieten, J.; Makrygiannis, E.; Blaschke, B.M.; Morandi, V.; Colombo, L.; Bonaccorso, F.; Garrido, J.A. High surface area graphene foams by chemical vapor deposition. *2D Mater.* **2016**, *3*, 45013. [[CrossRef](#)]
3. Drillet, J.-F.; Adams, M.; Barg, H.A.; Koch, D.; Schmidt, V. Development of a novel Zinc/air fuel cell with a Zn foam anode, a PVA/KOH membrane and a MnO<sub>2</sub>/SiOC-based air cathode. *ECS Trans.* **2010**, *28*, 13. [[CrossRef](#)]
4. Klabunde, K.J. Introduction to nanotechnology. *Nanoscale Mater. Chem.* **2001**, 1–13. [[CrossRef](#)]
5. Banhart, J.; Bellmann, D.; Clemens, H. Investigation of metal foam formation by microscopy and ultra small-angle neutron scattering. *Acta Mater.* **2001**, *49*, 3409–3420. [[CrossRef](#)]
6. Queheillalt, D.T.; Hass, D.D.; Sypeck, D.J.; Wadley, H.N.G. Synthesis of open-cell metal foams by templated directed vapor deposition. *J. Mater. Res.* **2001**, *16*, 1028–1036. [[CrossRef](#)]
7. Paserin, V.; Marcuson, S.; Shu, J.; Wilkinson, D.S. The chemical vapor deposition technique for Inco nickel foam production—manufacturing benefits and potential applications. *Cell. Met. Met. Foam. Technol.* **2003**, 31.

8. Yu, C.-J.; Eifert, H.H.; Banhart, J.; Baumeister, J. Metal foaming by a powder metallurgy method: Production, properties and applications. *Mater. Res. Innov.* **1998**, *2*, 181–188. [[CrossRef](#)]
9. Ozan, S.; Billhan, S. Effect of fabrication parameters on the pore concentration of the aluminum metal foam, manufactured by powder metallurgy process. *Int. J. Adv. Manuf. Technol.* **2008**, *39*, 257–260. [[CrossRef](#)]
10. Neville, B.; Rabiei, A. Composite metal foams processed through powder metallurgy. *Mater. Des.* **2008**, *29*, 388–396. [[CrossRef](#)]
11. Nagai, K.; Wada, D.; Nakai, M.; Norimatsu, T. Electrochemical Fabrication of Low Density Metal Foam with Mono-Dispersed-Sized Micro- and Submicro-Meter Pore. *Fusion Sci. Technol.* **2006**, *49*, 686–690. [[CrossRef](#)]
12. Gibson, L.; Ashby, M. *Cellular Solids*; Cambridge University Press: Cambridge, UK, 1997.
13. Banhart, J. Manufacture, characterisation and application of cellular metals and metal foams. *Prog. Mater. Sci.* **2001**, *46*, 559–632. [[CrossRef](#)]
14. Kulshreshtha, A.; Dhakad, S. Preparation of metal foam by different methods: A review. *Mater. Today Proc.* **2020**, *26*, 1784–1790. [[CrossRef](#)]
15. Kovacic, J.; Simancik, F. Comparison of inc and aluminium foam behaviour. *Transl. Ve Riečansky* **2004**, *42*, 79–90.
16. Liu, P.; Fu, C.; Li, T.; Shi, C. Relationship between tensile strength and porosity for high porosity metals. *Sci. China Technol. Sci.* **1999**, *42*, 100–107. [[CrossRef](#)]
17. Liu, P.; Liang, K. Preparation and corresponding structure of nickel foam. *Mater. Sci. Technol.* **2000**, *16*, 575–578. [[CrossRef](#)]
18. Liu, P.; Liang, K.; Tu, S.; Gu, S.; Yu, Q.; Li, T.; Fu, C. Relationship between tensile strength and preparation conditions for nickel foam. *Mater. Sci. Technol.* **2001**, *17*, 1069–1072. [[CrossRef](#)]
19. Liu, P.S. Effect of preparation conditions on relative elongation of nickel foam. *Mater. Sci. Technol.* **2004**, *20*, 669–672. [[CrossRef](#)]
20. Zhang, X.G. Fibrous zinc anodes for high power batteries. *J. Power Sources* **2006**, *163*, 591–597. [[CrossRef](#)]
21. Tian, Q.H.; Guo, X.Y.; Xue, P.; Song, Y.; Duan, L. Electro-Deposition for Foamed Zinc Material from Zinc Sulfate Solution. In *Materials Science Forum*; Trans Tech Publications Ltd.: Bäch, Switzerland, 2007; pp. 1669–1672.
22. Gupta, T.; Kim, A.; Phadke, S.; Biswas, S.; Luong, T.; Hertzberg, B.J.; Chamoun, M.; Evans-Lutterodt, K.; Steingart, D.A. Improving the cycle life of a high-rate, high-potential aqueous dualion battery using hyper-dendritic Zinc and copper hexacyanoferrate. *J. Power Sources* **2016**, *305*, 22–29. [[CrossRef](#)]
23. Wang, L.-P.; Li, N.-W.; Wang, T.-S.; Yin, Y.-X.; Guo, Y.-G.; Wang, C.-R. Conductive graphite fiber as a stable host for Zinc metal anodes. *Electrochim. Acta* **2017**, *244*, 172–177. [[CrossRef](#)]
24. Moreno-García, P.; Schlegel, N.; Zanetti, A.; Cedeño López, A.; Gálvez-Vázquez, M.A.D.J.S.; Dutta, A. Selective electrochemical reduction of CO<sub>2</sub> to CO on Zn-based foams produced by Cu<sup>2+</sup> and template-assisted electrodeposition. *ACS Appl. Mater. Interfaces* **2018**, *10*, 31355–31365. [[CrossRef](#)]
25. Quan, F.; Zhong, D.; Song, H.; Jia, F.; Zhang, L. A highly efficient zinc catalyst for selective electroreduction of carbon dioxide in aqueous NaCl solution. *J. Mater. Chem. A* **2015**, *3*, 16409–16413. [[CrossRef](#)]
26. Low, Q.H.; Loo, N.W.X.; Calle-Vallejo, F.; Yeo, B.S. Enhanced Electroreduction of Carbon Dioxide to Methanol Using Zinc Dendrites Pulse-Deposited on Silver Foam. *Angew. Chem. Int. Ed.* **2019**, *58*, 2256–2260. [[CrossRef](#)] [[PubMed](#)]
27. Stock, D.; Dongmo, S.; Miyazaki, K.; Abe, T.; Janek, J.; Schröder, D. Towards zinc-oxygen batteries with enhanced cycling stability: The benefit of anion-exchange ionomer for zinc sponge anodes. *J. Power Sources* **2018**, *395*, 195–204. [[CrossRef](#)]
28. Li, C.; Shi, X.; Liang, S.; Ma, X.; Han, M.; Wu, X.; Zhou, J. Spatially homogeneous copper foam as surface dendrite-free host for zinc metal anode. *Chem. Eng. J.* **2019**, *379*, 122248. [[CrossRef](#)]
29. Grisales, C.; Herrera, N.; Fajardo, F. Preparation of graphite conductive paint and its application to the construction of RC circuits on paper. *Phys. Educ.* **2016**, *51*, 055011. [[CrossRef](#)]
30. Phillips, C.; Al-Ahmadi, A.; Potts, S.-J.; Claypole, T.; Deganello, D. The effect of graphite and carbon black ratios on conductive ink performance. *J. Mater. Sci.* **2017**, *52*, 9520–9530. [[CrossRef](#)]
31. Ong, T.; Yang, H. Effect of atmosphere on the mechanical milling of natural graphite. *Carbon* **2000**, *38*, 2077–2085. [[CrossRef](#)]
32. Caicedo, F.M.C.; López, E.V.; Agarwal, A.; Drozd, V.; Durygin, A.; Hernandez, A.F.; Wang, C. Synthesis of graphene oxide from graphite by ball milling. *Diam. Relat. Mater.* **2020**, *109*, 108064. [[CrossRef](#)]
33. Kusumawati, D.H.; Nurhuda, M.; Santjojo, D.D.H.; Masrurroh, M. Graphite Particle Reduction Process using High Energy Milling. In Proceedings of the International Conference on Science and Technology (ICST 2018), Bali, Indonesia, 18–19 October 2018.
34. Chen, C.-N.; Chen, Y.-L.; Tseng, W.J. Surfactant-assisted de-agglomeration of graphite nanoparticles by wet ball mixing. *J. Mater. Process. Technol.* **2007**, *190*, 61–64. [[CrossRef](#)]
35. Antisari, M.; Montone, A.; Jovic, N.; Piscopiello, E.; Alvani, C.; Piloni, L. Low energy pure shear milling: A method for the preparation of graphite nano-sheets. *Scr. Mater.* **2006**, *55*, 1047–1050. [[CrossRef](#)]
36. Alofi, A.; Srivastava, G.P. Thermal conductivity of graphene and graphite. *Phys. Rev. B* **2013**, *87*. [[CrossRef](#)]
37. Zhao, W.; Fang, M.; Wu, F.; Wu, H.; Wang, L.; Chen, G. Preparation of graphene by exfoliation of graphite using wet ball milling. *J. Mater. Chem.* **2010**, *20*, 5817–5819. [[CrossRef](#)]
38. Sun, Y.; Lu, J.; Zhuang, L. Rational determination of exchange current density for hydrogen electrode reactions at carbon-supported Pt catalysts. *Electrochim. Acta* **2010**, *55*, 844–850. [[CrossRef](#)]
39. Gavilán-Arriazu, E.M.; Mercer, M.P.; Pinto, O.A.; Oviedo, O.A.; Barraco, D.E.; Hoster, H.E.; Leiva, E.P.M. Effect of Temperature on The Kinetics of Electrochemical Insertion of Li-Ions into a Graphite Electrode Studied by Kinetic Monte Carlo. *J. Electrochem. Soc.* **2019**, *167*, 013533. [[CrossRef](#)]

- 
40. Hosoi, T.; Yonekura, T.; Sunada, K.; Sasaki, K. Exchange Current Density of SOFC Electrodes: Theoretical Relations and Partial Pressure Dependencies Rate-Determined by Electrochemical Reactions. *J. Electrochem. Soc.* **2014**, *162*, F136–F152. [[CrossRef](#)]
  41. Teeratananon, M. Current Distribution Analysis of Electroplating Reactors and Mathematical Modeling of the Electroplated Zinc-Nickel Alloy. Ph.D. Thesis, National Polytechnic Institute of Toulouse, Toulouse, France, 2004.